Secondary Au−Au and Sn−Sn Interactions in the Superstructure of YbAuSn—Missing Link in the Series of KHg_2 Superstructures

Rolf-Dieter Hoffmann, Rainer Pöttgen,* and Dirk Kussmann

Department Chemie, Ludwig-Maximilians-Universität München, Butenandtstrasse 5−13 (Haus D), D-81377 München, Germany

Ralf Müllmann and Bernd D. Mosel*

Institut für Physikalische Chemie, Universität Münster, Schlossplatz 4/7, D-48149 Münster, Germany

Received March 14, 2001. Revised Manuscript Received May 22, 2001

The stannide YbAuSn has been synthesized in quantitative yield by reacting the elements in sealed tantalum tubes in a high-frequency furnace. The structure was determined from single-crystal X-ray data: *Imm*2, $a = 469.7(1)$ pm, $b = 2191.2(4)$ pm, $c = 812.7(1)$ pm, wR2 = 0.111, 2061 F^2 values, and 58 variables. It crystallizes with a pronounced KHg_2 type subcell (*a*, 1/3*b*, *c*, *Imma*). In the superstructure the tripled *b* axis allows an ordered stacking of Au_3Sn_3 hexagons with weak gold−tin, gold−gold, and tin−tin interlayer bonding interactions. The determined stacking sequence − + − − + −, − + − − + − in YbAuSn realizes a so far missing sequence within a general ordering scheme of KHg_2 type superstructures. The group−subgroup relation in going from the KHg_2 subcell and chemical bonding in YbAuSn are discussed. Each ytterbium site has an ordered near-neighbor environment of six gold and six tin atoms in the form of two tilted hexagons. Magnetic susceptibility measurements show a nonmagnetic ground state of the ytterbium atoms. YbAuSn is a metallic conductor with a specific resistivity of 50 $\mu\Omega$ cm at room temperature. ^{119}Sn Mössbauer spectroscopic data show one signal at an isomer shift of 1.922(5) mm/s subjected to quadrupole splitting of 0.929(9) mm/s.

Introduction

The equiatomic gold stannides RAuSn (R = alkaline earth or rare earth metal) exhibit an unusually large structural variety. With the trivalent rare earth metals we observe the hexagonal NdPtSb type (R = Y, Ce−Nd, Sm, Gd−Ho) and the cubic MgAgAs type (R = Sc, Ho, Er, Tm, Lu) structures.[1−3] Among these stannides, HoAuSn is dimorphic.[1] The volume per formula unit is smaller for the NdPtSb modification (67.9 Å^3) than for the MgAgAs modification (72.7 Å^3). Detailed investigations of the magnetic properties[4−14] clearly revealed the trivalent oxidation state for the rare earth atoms in these intermetallics. The [AuSn] polyanions of these compounds consist of slightly puckered, two-dimensional Au_3Sn_3 hexagons (NdPtSb type) or a three-dimensional network of corner-sharing $AuSn_{4/4}$ tetrahedra (MgAgAs type). No Au−Au nor Sn−Sn interactions occur in these polyanions.

This situation becomes totally different when an alkaline earth or a potentially divalent rare earth metal is introduced. So far, the structures of MgAuSn,[2,15] CaAuSn,[16] and EuAuSn[17] have been solved. While the cubic MgAgAs type is still formed with the small magnesium atoms, CaAuSn[16] and EuAuSn[17] adopt two different complex superstructures of the KHg_2 type. In both cases weak superstructure reflections forced a quintupling of the unit cells. The superstructures result from a different coloring of the gold and tin atoms on

* Corresponding authors. E-mail rapch@cup.uni-muenchen.de and mosel@uni-muenster.de.

(1) Dwight, A. E. *Proc. Rare Earth Res. Conf. 12th* **1976**, *1*, 480.
(2) Eberz, U.; Seelentag, W.; Schuster, H.-U. *Z. Naturforsch. B* **1980**, *35*, 1341.
(3) Canepa, F.; Cirafici, S. *J. Alloys Compd.* **1996**, *232*, 71.
(4) Oesterreicher, H. *J. Less-Common Met.* **1977**, *55*, 131.
(5) Lenkewitz, M.; Corsepius, S.; Stewart, G. R. *J. Alloys Compd.* **1996**, *241*, 121.
(6) Baran, S.; Hofmann, P.; Leciejewicz, J.; Ślaski, M.; Szytuła, A.; Zygmunt, A. *J. Phys. C: Cond. Matter* **1997**, *9*, 9053.
(7) Bialic, D.; Kruk, R.; Kmieć, R.; Tomala, K. *J. Alloys Compd.* **1997**, *257*, 49.
(8) Adroja, D. T.; Rainford, B. D.; Neville, A. J. *J. Phys. C: Cond. Matter* **1997**, *9*, L391.
(9) Łątka, K.; Görlich, E. A.; Chajek, W.; Kmieć, R.; Pacyna, A. W. J. *J. Alloys Compd.* **1997**, *262−263*, 108.
(10) Baran, S.; Leciejewicz, J.; Ślaski, M.; Hofmann, P.; Szytuła, A. *J. Alloys Compd.* **1998**, *275−277*, 541.
(11) Görlich, E. A.; Łątka, K.; Kmieć, R.; Warkocki, W. *Mol. Phys. Rep.* **1998**, *22*, 35.
(12) Łątka, K.; Görlich, E. A.; Kmieć, R.; Kruk, R.; Pacyna, A. W. J.; Chajek, W. *Mol. Phys. Rep.* **1998**, *22*, 87.
(13) Chajek, W.; Łątka, K.; Kmieć, R.; Kruk, R.; Pacyna, A. W. J. *Mol. Phys. Rep.* **1998**, *22*, 117.
(14) Oner, Y.; Senoussi, S.; Sologub, O.; Salamakha, P. *Physica B* **1999**, *259−261*, 887.
(15) Pulm, H.; Hohlneicher, G.; Freund, H. J.; Schuster, H.-U.; Drews, J.; Eberz, U. *J. Less-Common Met.* **1986**, *115*, 127.
(16) Kuβmann, D.; Hoffmann, R.-D.; Pöttgen, R. *Z. Anorg. Allg. Chem.* **1998**, *624*, 1727.
(17) Pöttgen, R.; Hoffmann, R.-D.; Müllmann, R.; Mosel, B. D.; Kotzyba, G. *Chem. Eur. J.* **1997**, *3*, 1852.

10.1021/cm011089q CCC: $20.00
Published on Web 10/09/2001

the subcell mercury positions. In both structures we observe puckered Au_3Sn_3 hexagons that are stacked in a different manner, resulting in interlayer Au−Sn as well as Au−Au and Sn−Sn bonding. The formation of the Au−Au interactions (relativistic nature of the gold atoms)[18] and the tin dumb-bells is certainly a driving force for the formation of the superstructures. Also SrAuSn[19] and BaAuSn[20] crystallize with pronounced KHg_2 subcells. The work on these superstructures is in progress.

We recently developed a general group−subgroup scheme for the classification of different KHg_2 superstructures (ATX; A = alkaline earth, rare earth; T = transition metal; X = main group element).[16,21] From a crystal chemical point of view the various KHg_2 superstructures can be categorized on the basis of stacking sequences of transition metal filled trigonal prisms formed by the X atoms. The scheme allows one to readily precalculate and predict superstructures of the KHg_2 type, i.e., the space group and the atomic coordinates. Helpful is that some of the KHg_2 type superstructures can be divided into two groups: (i) body-centered groups based upon *Imm*2 (EuAuGe[22] derivative) and (ii) primitive groups based upon *Pnma* (TiNiSi[23] derivative). With other words all EuAuGe variants are noncentrosymmetric and body-centered, while the TiNiSi variants are primitive and centrosymmetric. This limitation into two groups has its cause in the requirement of a reasonable crystal chemistry. The group−subgroup relations itself naturally allow an infinite number of superstructures, but taking the available data this is so far limited to only isomorphic (i) symmetry reductions.

The crystal chemistry expresses itself by stacking transition metal filled trigonal prisms and introducing weak interlayer bonding interactions between gold−gold, tin−tin, and gold−tin contacts, thus fine-tuning the structure. The prisms are labeled + if they point in the +*z* direction and − for the opposite.[17] In this scheme, an ordered variant with space group *Imm*2 and a tripled unit cell was missing.[16,21] A slight drawback is that the theoretical stacking sequences are not necessarily unambiguous. For the tripled unit cell, six prisms have to be aligned, for which two sequences are possible: + + − − + +, + + − − + + or − + − − + −, − + − − + −. The difference lies only in converting the first prism from + to −, which means an exchange of gold and tin atoms for that prism. In the present paper we report on the structure determination of YbAuSn, which turned out to be the *missing link*. YbAuSn has already been reported in the literature,[24,25] but the wrong structure type has been assigned. On the basis of X-ray powder data it was concluded that YbAuSn is isotypic with the TiNiSi type. In these investigations, the weak superstructure reflections have most likely been overlooked. In addition to the precise structure determination, we report also on magnetic susceptibility, electrical resistivity, and ^{119}Sn Mössbauer spectroscopic measurements.

Experimental Procedures

Synthesis. Starting materials for the syntheses of YbAuSn were ingots of ytterbium (Heraeus), gold wire (Ø 1 mm, Degussa), and a tin bar (Heraeus), all with stated purities better than 99.9%. Homogeneous samples of YbAuSn were obtained via two different synthesis techniques. In the first experiment the elements (ideal 1:1:1 starting composition) were reacted in glassy carbon crucibles (Sigradur G, glassy carbon, type GAZ006) under flowing argon in a high-frequency furnace (Hüttinger Elektronik, Freiburg, Typ TIG 1.5/300). The argon was purified over silica gel, molecular sieves, and titanium sponge (900 K). The glassy carbon crucibles were placed in a water-cooled sample chamber as described in detail elsewhere.[16] During the inductive heating process, gold and tin first form an alloy at low temperature that finally reacts with the ytterbium pieces in a strongly exothermic reaction. To ensure homogeneity and good crystallization, the sample was held for 2 h at ∼800 K. No weight losses were observed for these reactions. After cooling to room temperature, the sample could easily be separated from the glassy carbon crucible by pounding at its base.

Alternatively, the elemental components were reacted in a sealed tantalum tube[26] in a quartz glass sample chamber of a high-frequency furnace (Kontron Roto-Melt, 1.2 kW) under flowing argon.[27] The tube was first heated with the maximum power output (about 1700 K) until the reaction started, which was indirectly visible by a heat flash. Then the sample was held at about 1400 K for another 2−3 min, followed by quenching. To ensure good crystallinity and to further check for possible reconstructive phase transitions, two more samples in tantalum tubes were prepared following the above syntheses conditions, but additionally the tantalum tubes were sealed in evacuated silica tubes and annealed for 10 days at 1170 K in conventional resistance furnaces. The second sample was kept for another 35 days at 870 K. After the annealing procedures the samples were cooled to room temperature by radiative heat loss. The samples could easily be separated from the tantalum tubes by mechanical fragmentation.

In both synthesis techniques no reactions of the samples with the crucible material could be detected. Polycrystalline samples and powders of YbAuSn are stable in moist air. No deterioration was observed after several months. Single crystals exhibit metallic luster and powders are dark gray.

The samples were routinely investigated by EDX analyses using a Leica 420 I scanning electron microscope with YbF_3, gold, and tin as standards. The compositions were all close to the ideal value. No impurity elements heavier than sodium ($Z = 11$) could be detected.

Structural Characterization. The samples were routinely characterized through Guinier powder patterns or powder diffractograms (Stoe Stadi P) using Cu Kα1 radiation and α-quartz (a = 491.30 pm, c = 540.46 pm) as an internal standard. The strongest reflections could be indexed hexagonally according to the AlB_2 type with $a = 470.0$ and $c = 365.2$ pm. Peak broadening and additional medium strong reflections led to an orthorhombic indexing with the lattice parameters a, $2c$, and $\sim a\sqrt{3}$, satisfying the extinction conditions of a body-centered lattice. The latter corresponds to a KHg_2[28] type subcell (space group *Imma*) with $a' = 469.7$, $b' = 730.4$, and $c' = 812.7$ pm with an $a'\sqrt{3}/c$ ratio of 1.001, very close to the ideal value of an orthohexagonal setting. Additional very weak reflections, confirmed by the single crystal work to belong to YbAuSn (see

(18) Schmidbaur, H. (Ed.) *Gold−Progress in Chemistry, Biochemistry and Technology*; Wiley: Chichester, 1999.
(19) Kuβmann, D.; Pöttgen, R. *Z. Kristallogr.* **1999**, *Suppl. 16*, 45.
(20) Hoffmann, R.-D.; Pöttgen, R.; Kussmann, D.; Niepmann, D.; Trill, H.; Mosel, B. D. *Solid State Sci.*, submitted.
(21) Hoffmann, R.-D.; Pöttgen, R. *Z. Kristallogr.* **2001**, *216*, 127.
(22) Pöttgen, R. *J. Mater. Chem.* **1995**, *5*, 505.
(23) Shoemaker, C. B., Shoemaker, D. P. *Acta Crystallogr.* **1965**, *18*, 900.
(24) Katoh, K.; Takabatake, T.; Minami, A.; Oguro, I.; Sawa, H. *J. Alloys Compd.* **1997**, *261*, 32.
(25) Kaczorowski, D.; Leithe-Jasper, A.; Rogl, P.; Flandorfer, H.; Cichorek, T.; Pietri, R.; Andraka, B. *Phys. Rev. B* **1999**, *60*, 422.
(26) Pöttgen, R.; Gulden, Th.; Simon, A. *GIT Labor-Fachzeitschrift* **1999**, *43*, 133.
(27) Pöttgen, R.; Lang, A.; Hoffmann, R.-D.; Künnen, B.; Kotzyba, G.; Müllmann, R.; Mosel, B. D.; Rosenhahn, C. *Z. Kristallogr.* **1999**, *214*, 143.

Table 1. Crystal Data and Structure Refinement for YbAuSn

empirial formula	YbAuSn
molar mass	488.7 g/mol
lattice parameters	$a = 469.7(1)$ pm
(Guinier data)	$b = 2191.2(4)$ pm
	$c = 812.7(1)$ pm
	$V = 0.8364(2)$ nm^3
formula units per cell	$Z = 12$
space group	*Imm*2 (No. 44)
calculated density	11.64 g/cm^3
crystal size	$20 \times 30 \times 40$ μm^3
transmission (max: min)	3.91
absorption coefficient	94.3 mm^{-1}
F(000)	2388
θ range	2−35°
range in *hkl*	±7, ±35, ±13
total no. reflections	8068
independent reflections	2061 ($R_{int} = 0.1099$)
reflections with $I > 2\sigma(I)$	1124 ($R_\sigma = 0.0718$)
data/restraints/parameters	2061/2/58
goodness-of-fit on F^2	0.974
final *R* indices [$I > 2\sigma(I)$]	R1 = 0.0449; wR2 = 0.0895
indices (all data)	R1 = 0.1098; wR2 = 0.1114
R indices (subcell reflections)[a]	616 > $2\sigma(I)$, $R = 0.0282$
R indices (supercell reflections)[a]	508 > $2\sigma(I)$, $R = 0.1051$
extinction coefficient	0.00036(3)
absolute structure parameter	0.00(3)
largest diff peak and hole	3.81 and −4.11 e/Å^3

[a] These values were calculated with the program RWERT[47] using the formula $R = \Sigma|F_o - F_c|/\Sigma|F_o|$.

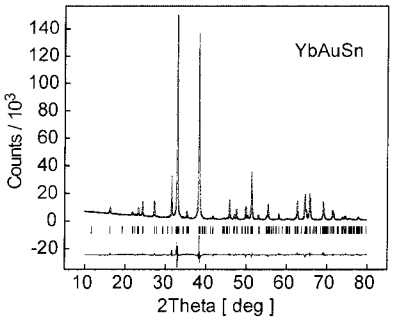

Figure 1. Powder diffractometer measurement and Rietveld refinement of YbAuSn (Cu Kα1 radiation).

below), forced a tripling of the subcell *b* axis, resulting in the lattice parameters listed in Table 1. To ensure correct indexing, the observed patterns were compared with a calculated one,[29] taking the positions of the refined structure. Powder diffractograms were taken of three samples: the 1400 K high-temperature sample as well as the at 1170 and 870 K annealed samples. Rietveld refinements with the FULLPROF program[30] using the positional parameters of the single crystal work for all three diffractograms revealed basically the same results and were in accordance with the single crystal work, except for larger standard deviations: YbAuSn derives from the aristotype AlB_2 and adopts a superstructure of the KHg_2 type with a tripled *b* axis. This is at least verified for the examined temperature range from 800 up to 1400 K, but it can be assumed that YbAuSn adopts the found superstructure over the whole temperature range. Exemplary, the Rietveld fit of the powder pattern of the 1170 K sample is shown in Figure 1.

Several small, irregularly shaped single crystals of YbAuSn could be isolated from the annealed samples by mechanical fragmentation. They were intensively investigated on a Buerger precession camera in order to establish both symmetry and suitability for intensity data collection. A set of layer photographs was taken from three crystals originating from the 800, 1170, and 1400 K sample.

Intensity data were recorded at room temperature by use of a four-circle diffractometer (CAD4) with graphite-monochromatized Mo Kα radiation ($\lambda = 71.073$ pm) and a scintillation counter with pulse-height discrimination. The scans were taken in the $\omega/2\theta$ mode and empirical absorption corrections were applied on the basis of ψ-scan data.

It turned out that two crystals (800 and 1400 K) consisted of trilling domains, as could be expected from the $\sqrt{3}$ ratio already determined from the powder patterns. Not being aware of the presence of trillings misleads one to falsely double lattice parameters (2*a* and 2*c*) and acknowledge nonspecific space group extinctions (i.e., a mainly and systematically empty reciprocal space). Some layers, however, still show nonspecific extinctions conditions, but they do not translate. This pronounced pseudosymmetry is characteristic of all KHg_2 superstructures. Doubling of *a* and *c* can safely be ruled out by looking at the subgroups of *Imma*. No such symmetry reduction is allowed for a space group with an *I* lattice. The only possible space group satisfying the observed extinction conditions is *Imm*2, which is nicely in accordance with the predicted one.

Initially the structure was solved for a trilling with space group *Imm*2 and the atomic positions deduced for the missing link. The correct stacking sequence for YbAuSn was found to be the aforementioned second choice: − + − − + −, − + − − + −. The refinement unfortunately was clearly hampered by large correlations of the anisotropic displacement parameters and the extra hindrance that, along with the trilling domains, twinning by inversion obviously had to be accounted for. The occurrence of twins of trillings (i.e. six domains with the refined ratios of 1:0.254:0.248:0.118:0.105:0.087) is understandable by the group−subgroup[31,32] relations (ref 21 and Figure 2), which contains two *translationengleiche* symmetry reductions of index three (t3) and of index two (t2). This refinement resulted in R1 = 0.094, wR2 = 0.179, 9205 F^2 values ($0\sigma_{F_o}$), and 63 parameters; R1 = 0.049 for 5694 F^2 values ($4\sigma_{F_o}$).

At the end an obviously single-domain crystal of YbAuSn was found in the 1170 K sample. Data collections and refinements were carried out on a step by step basis given by the group−subgroup relations presented in Figure 2. To check for possible trilling reflections the strongest superstructure reflections of YbAuSn were calculated taking the parameters of the above refinement. No measurable intensities could be observed at those positions in reciprocal space corresponding to trilling reflections. Therefore, at first a complete data set was collected only for the KHg_2 type subcell (*Imma*, $a = 470$, $b = 730$, and $c = 812.7$ pm). This refinement resulted in R1 = 0.029 (352 F^2 and 12 parameters) with the expected mixed Au/Sn occupancy. The refined parameters are used in Figure 2. Following the group−subgroup relations the next refinement was carried out based on the superstructure of the EuAuGe type[22] (space group *Imm*2), which would principally allow ordering of gold and tin atoms. As is shown in Figure 2, ordering of gold and tin was not possible. Instead mixed occupancies of 0.66 Au/0.33 Sn and 0.33 Au/0.66 Sn were found for the two positions (R1 = 0.024, 386 F^2, and 23 parameters). The latter result could also be expected, because the weak superstructure reflections have purposely been ignored.

In the final step a complete data set including the very weak superstructure reflections causing the *b* axis to be tripled was collected by employing a longer counting time (180 s per reflection) to ensure a reasonable good counting statistic.

The starting atomic parameters were assigned on the basis of the precalculated ones, and the structure was successfully

(28) Duwell, E. J., Baenziger, N. C. *Acta Crystallogr.* **1955**, *8*, 705.
(29) Yvon, K.; Jeitschko, W.; Parthé, E. *J. Appl. Crystallogr.* **1977**, *10*, 73.
(30) Rodriguez-Carvajal, J., *FULLPROF 3.5, Rietveld, Profile Matching and Integrated Intensity Refinement of X-ray Data and/or Neutron Data*, Institut Laue-Langevin, 2000 (unpublished).
(31) Bärnighausen, H. *Commun. Math. Chem.* **1980**, *9*, 139.
(32) Bärnighausen, H., Müller, U. *Symmetriebeziehungen zwischen den Raumgruppen als Hilfsmittel zur straffen Darstellung von Strukturzusammenhängen in der Kristallchemie,* University of Karlsruhe and University Gh. Kassel, Germany, 1996.

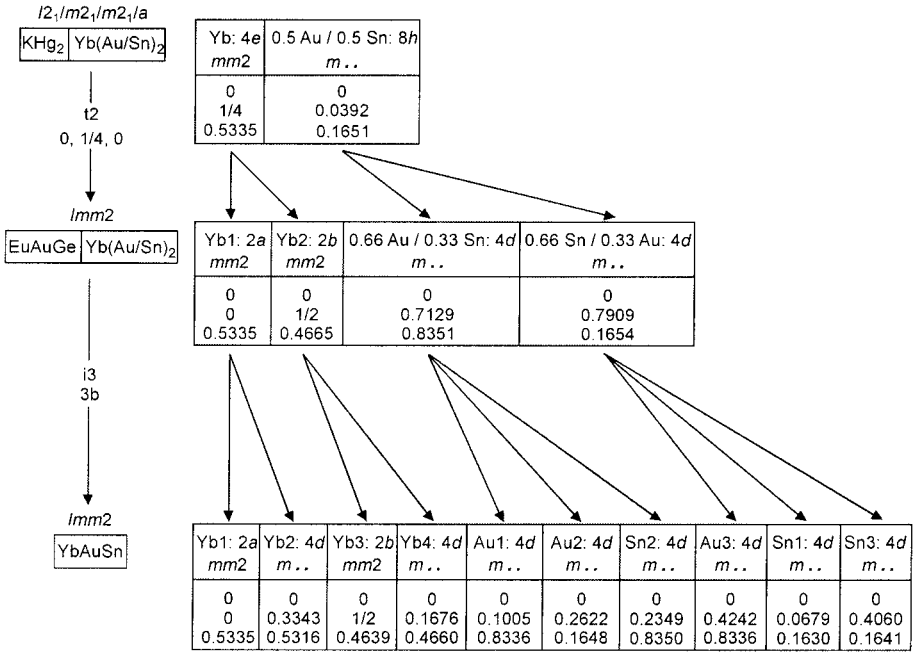

Figure 2. Bärnighausen tree for the group−subgroup relations of the KHg_2 type subcell of $Yb(Au/Sn)_2$ and ordered YbAuSn via the EuAuGe type. The evolution of the atomic sites together with the index of the *translationengleiche* (t) and the isomorphic (i) symmetry reduction is given as well as the origin shift.

Table 2. Atomic Coordinates and Isotropic Displacement Parameters for YbAuSn

atom	Wyckoff position	*x*	*y*	*z*	U_{eq}[a]
Yb1	2a	0	0	0.5335(5)	140(7)
Yb2	4d	0	0.33430(9)	0.5316(3)	108(5)
Yb3	2b	0	1/2	0.4639(5)	123(6)
Yb4	4d	0	0.16763(9)	0.4660(3)	123(5)
Au1	4d	0	0.10052(9)	0.8336(4)	113(4)
Au2	4d	0	0.2622(1)	0.1648(3)	143(4)
Au3	4d	0	0.42420(9)	0.8336(4)	117(4)
Sn1	4d	0	0.0679(2)	0.1630(6)	98(6)
Sn2	4d	0	0.2349(2)	0.8350(5)	82(4)
Sn3	4d	0	0.4060(2)	0.1641(6)	179(8)

[a] U_{eq} (pm^2) is defined as one-third of the trace of the orthogonalized U_{ij} tensor.

refined with anisotropic displacement parameters using SHELXL-97[33] (full-matrix least-squares on F^2). The refinements readily converged to the residuals listed in Table 1 and a subsequent difference Fourier synthesis revealed no significant residual peaks. Especially the Flack[34,35] parameter gave no indication of twinning by inversion, which is possible due to the translationengleiche symmetry reduction of index two (t2) in going from the KHg_2 to the EuAuGe type. All relevant crystallographic details are listed in Table 1. Atomic coordinates and interatomic distances are given in Tables 2 and 3. Listings of the anisotropic displacement parameters and the structure factors are available.[36]

As a check for the correct compositions, the occupancy parameters were varied in a separate series of least-squares cycles along with the displacement parameters. All sites were fully occupied within two to five standard deviations, and in the final cycles the ideal composition was assumed. The X-ray data gave no hint for gold/tin mixing within the polyanion.

Physical Property Investigations. The magnetic susceptibilities of polycrystalline pieces of YbAuSn were determined with a SQUID magnetometer (Quantum Design, Inc.) in the temperature range from 4.2 to 300 K with magnetic flux densities up to 5.5 T. The specific resistivities were

Table 3. Interatomic Distances (pm) in the Structure of YbAuSn[a]

Yb1:	2	Au1	328.6	Yb3:	2	Sn3	319.1
	4	Sn3	329.9		4	Sn1	321.7
	4	Au3	330.3		4	Au1	338.9
	2	Sn1	335.9		2	Au3	343.4
	2	Yb4	371.4		2	Yb2	367.2
	2	Yb3	421.3		2	Yb1	421.3
Yb2:	1	Au3	314.8	Yb4:	1	Au2	320.8
	2	Au1	318.5		2	Au2	323.9
	2	Sn2	322.0		2	Sn3	327.2
	1	Sn2	329.1		2	Au3	327.4
	2	Au2	334.1		1	Sn1	329.2
	2	Sn1	335.4		1	Au1	333.0
	1	Au2	337.3		1	Sn2	334.2
	1	Sn3	337.4		2	Sn2	334.8
	1	Yb3	367.2		1	Yb2	369.1
	1	Yb4	369.1		1	Yb1	371.4
	2	Yb4	424.1		2	Yb2	424.1
Au1:	2	Sn3	272.6	Sn1:	2	Au3	273.3
	1	Sn1	277.1		1	Au1	277.1
	1	Sn2	294.4		1	Sn1	297.6
	2	Yb2	318.5		2	Yb3	321.7
	1	Yb1	328.6		1	Yb4	329.2
	1	Yb4	333.0		2	Yb2	335.4
	2	Yb3	338.9		1	Yb1	335.9
Au2:	2	Sn2	272.6	Sn2:	2	Au2	272.6
	1	Sn2	274.6		1	Au2	274.6
	1	Sn3	315.0		1	Au1	294.4
	1	Yb4	320.8		2	Yb2	322.0
	2	Yb4	323.9		1	Yb2	329.1
	2	Yb2	334.1		1	Yb4	334.2
	1	Yb2	337.3		2	Yb4	334.8
Au3:	1	Sn3	271.5	Sn3:	1	Au3	271.5
	2	Sn1	273.3		2	Au1	272.6
	1	Yb2	314.8		1	Au2	315.0
	2	Yb4	327.4		1	Yb3	319.1
	2	Yb1	330.3		2	Yb4	327.2
	1	Au3	332.2		2	Yb1	329.9
	1	Yb3	343.4		1	Yb2	337.4

[a] All distances of the first coordination spheres are listed. Standard deviations are all equal or less than 0.4 pm.

(33) Sheldrick, G. M. SHELXL-97, Program for Crystal Structure Refinement, University of Göttingen, Germany, 1997.
(34) Flack, H. D., Bernadinelli, G. *Acta Crystallogr.* **1999**, *A 55*, 908.
(35) Flack, H. D., Bernadinelli, G. *J. Appl. Crystallogr.* **2000**, *33*, 1143.
(36) Details may be obtained from: Fachinformationszentrum Karlsruhe, D-76344 Eggenstein-Leopoldshafen (Germany), by quoting the Registry No. CSD-411776. E-mail: crysdata@fiz-karlsruhe.de.

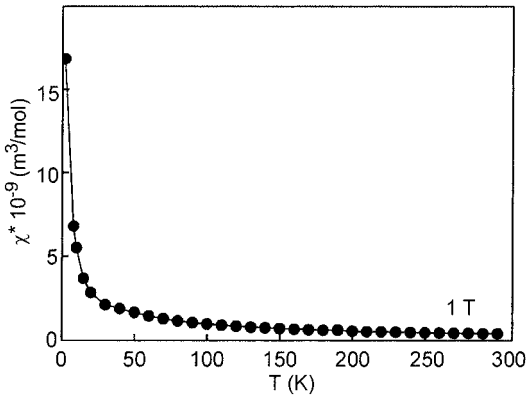

Figure 3. Temperature dependence of the magnetic susceptibility of YbAuSn measured at a flux density of 1 T.

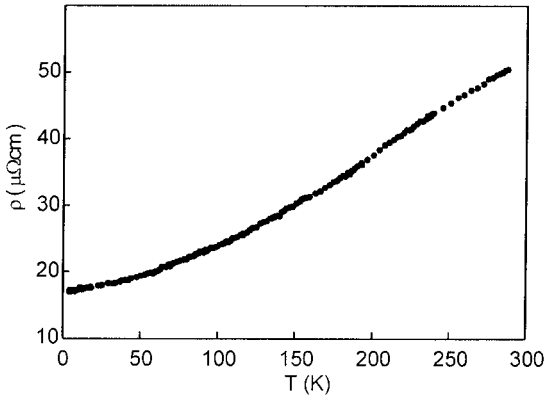

Figure 4. Temperature dependence of the specific resistivity of YbAuSn.

measured on small, irregularly shaped polycrystalline blocks (typical dimensions 1 × 1 × 2 mm^3) using a four-probe technique. Cooling and heating curves measured between 4.2 and 300 K were identical within the error limits, also for different samples. ^{119}Sn Mössbauer spectroscopic experiments were performed with a $Ca^{119m}SnO_3$ source at 300 K on the same polycrystalline samples used for the magnetic and electrical measurements. A palladium foil of 0.05 mm thickness was used to reduce the thin K X-rays concurrently emitted by the source.

Results and Discussion

Magnetic Properties. The temperature dependence of the magnetic susceptibility of YbAuSn is displayed in Figure 3. The susceptibilities were only weakly dependent on the external field, indicating only very small amounts of ferromagnetic impurities. The 1 T (Figure 3) and 3 T data were practically identical. Down to about 50 K the susceptibilities are very small and nearly independent of temperature. The upturn below 50 K may be attributed to a minor degree of paramagnetic impurities, although our Guinier diagrams showed single-phase YbAuSn. The susceptibility at 300 K is 0.4(1) × 10^{-9} m^3/mol, indicating Pauli paramagnetism. This is in agreement with the metallic behavior discussed below. Our magnetic data entirely match the previous investigations by Katoh et al.[24] and Kaczorowski et al.[25]

Electrical Properties. The temperature dependence of the specific resistivity of YbAuSn is presented in Figure 4. The specific resistivity decreases with decreasing temperature as expected for a metal. The room-temperature value is 50 ± 10 μΩ cm. The relatively large error limit accounts for the different values obtained for several irregularly shaped samples. At 4.2 K the specific resistivity has dropped to 17 ± 5 μΩ cm, resulting in a resistivity ratio of ρ(4.2 K)/ρ(300 K) = 0.34. Over the whole temperature range, no anomaly could be observed. The shape of the resistivity curve presented by Katoh et al.[24] is slightly different. This is most likely due to the polycrystalline character of both samples.

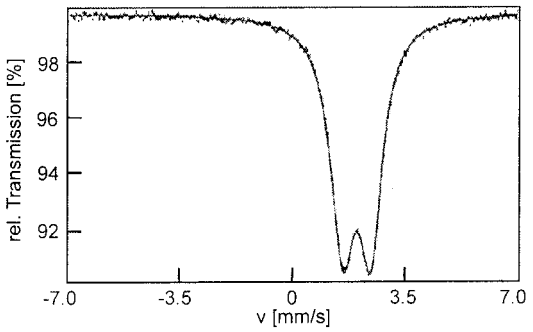

Figure 5. Experimental and simulated ^{119}Sn Mössbauer spectrum of YbAuSn at 4.2 K.

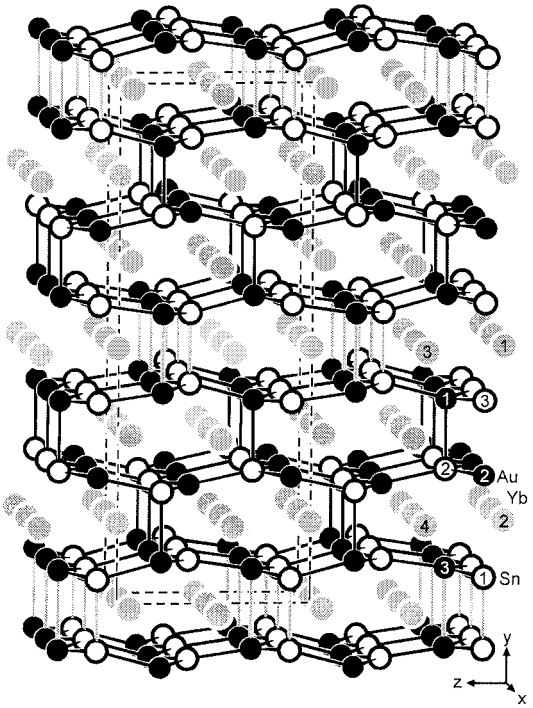

Figure 6. Crystal structure of YbAuSn. Ytterbium, gold, and tin atoms are drawn as gray, black filled, and open circles, respectively. Single digits correspond to the atom designations. Along with the unit cell the three-dimensional [AuSn] polyanion is outlined. The different bonding interactions within the hexagons and between the stacked layers are emphasized by black and gray lines. For details, see the text.

^{119}Sn Mössbauer Spectroscopy. The ^{119}Sn Mössbauer spectrum at 4.2 K of YbAuSn is shown in Figure 5 together with a theoretical transmission integral fit. Despite the three crystallographically different tin sites, the spectrum could be fit with one signal at an isomer shift of δ = 1.922(5) mm/s subjected to quadrupole splitting of ΔE_Q = 0.929(2) mm/s. The experimental line width is Γ = 1.05(5) mm/s. Since the coordinations of the Sn1, Sn2, and Sn3 atoms are quite similar, the

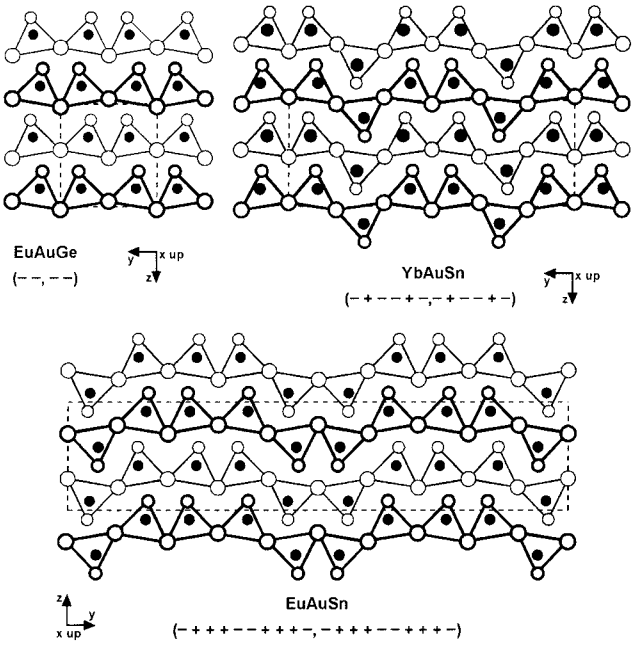

Figure 7. Projections of the crystal structures of EuAuGe, YbAuSn, and EuAuSn along the short axes: Eu and Yb, large open circles; Au, filled circles; Ge and Sn, small open circles. All atoms are situated on mirror planes at $x = 0$ and $x = 1/2$, indicated by thin and thick lines, respectively. The gold centered trigonal prisms are outlined. The orientations of the prisms are labeled + if they point in the $+z$ direction and − if they point in the $-z$ direction.

respective Mössbauer signals are most likely indistinguishable. Thus, the doublet is a superimposed signal of three very similar doublets. Such a composed ^{119}Sn Mössbauer spectrum was observed recently also for the stannides $CeRhSn_2$[37] and $Ce_3Pd_4Sn_6$.[38]

Crystal Chemistry and Chemical Bonding. The superstructure of YbAuSn is reported here for the first time. It derives from the well-known hexagonal aristotype AlB_2. YbAuSn (Figures 6−8) crystallizes with a pronounced KHg_2 type subcell. Orthorhombic KHg_2 itself forms a branch of the AlB_2 symmetry tree[21] and represents a large number of intermetallic compounds.[39] Equiatomic YbAuSn belongs to this family and forms a peculiar superstructure. It fits well into a general scheme developed for systemizing KHg_2 type superstructures.[16,17] Stacking sequences are as follows for EuAuGe variants: − −, − − for EuAuGe, − + − − + −, − + − − + − for YbAuSn, and − + + + − − + + + −, − + + + − − + + + − for EuAuSn,[17] They are the following for TiNiSi variants: − +, − + for EuAuIn, − − − + + +, − − − + + + for CaCuGe, and − − + − − + + − + +, − − + − − + + − + + for CaAuSn.[16]

In AlB_2-type EuCuGe,[40,41] each europium is sandwiched by two $(Cu/Ge)_6$ hexagons and additionally has six europium neighbors within the hexagonal plane and

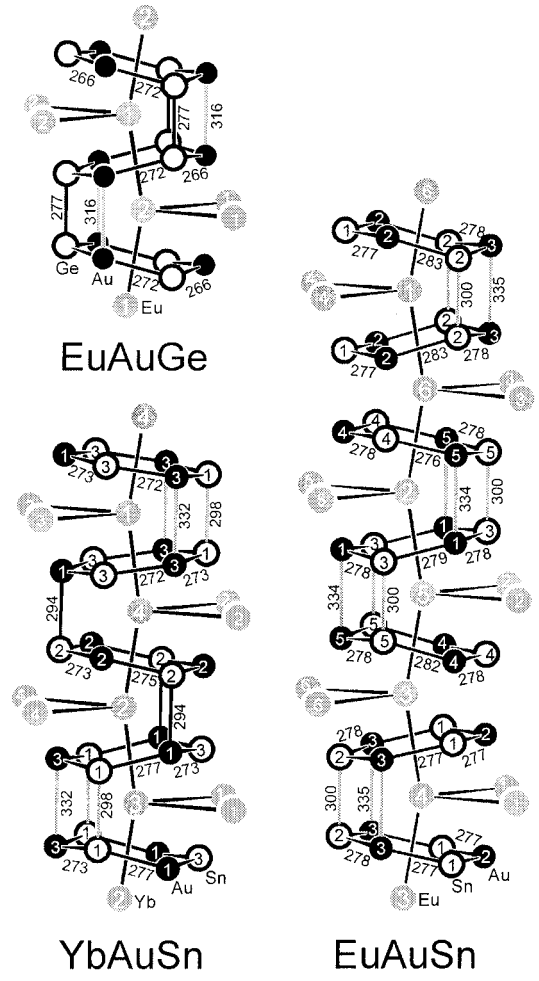

Figure 8. Near-neighbor environments of EuAuGe, YbAuSn, and EuAuSn. Single digits correspond to the atom designations. Bond lengths are given in pm. For details, see the text.

two further europiums on the hexagonal axis. This highly symmetrical arrangement happens to distort heavily in going to the orthorhombic AlB_2 derivatives KHg_2[28] and EuAuGe.[22] KHg_2 does not allow ordering on the mercury positions, while the gold and germanium atoms are ordered within the hexagons of EuAuGe. The structure of EuAuGe can be seen as the simplest superstructure of KHg_2 next to the many TiNiSi[23,39] variants. EuAuSn[17] and YbAuSn derive from EuAuGe and they constitute variations of the coloring of the hexagons by gold and tin atoms. The various coloring schemes lead to different near-neighbor environments for the four ytterbium atoms of YbAuSn (Figure 8). The net number of neighbors is the same for each ytterbium atom except the positioning of gold and tin atoms varies. The latter has a great effect on the three-dimensional character of the [AuSn] polyanion (Figures 6 and 8). Along with the gold/tin coloring goes the insertion of interlayer contacts of tin−tin (298) and weak gold−tin (294 pm) and gold−gold (332 pm) bonding interactions. In contrast, the intralayer gold−tin distances are the shortest contacts and are on average 273 pm, very close to the sum of Pauling's single bond radii of 274 pm for gold and tin.[42] They are comparable to the slightly

(37) Niepmann, D., Pöttgen, R., Künnen, B., Kotzyba, G., Rosenhahn, C., Mosel, B. D. *Chem. Mater.* **1999**, *11*, 1597.
(38) Niepmann, D., Pöttgen, R., Künnen, B., Kotzyba, G.; Mosel, B. D. *Chem. Mater.* **2000**, *12*, 533.
(39) Villars, P., Calvert, L. D. *Pearson's Handbook of Crstallographic Data for Intermetallic Phases*; American Society for Metals, Metals Park, OH 44073, USA, 1991.
(40) Pöttgen, R. *Z. Kristallogr.* **1996**, *211*, 884.
(41) Pöttgen, R.; Johrendt, D. *Chem. Mater.* **2000**, *12*, 875.
(42) Pauling, L. *The Nature of the Chemical Bond and the Structures of Molecules and Solids*; Cornell University Press: Ithaca, NY, 1960.

longer average gold−tin distances found in NaAuSn (275)[43] and EuAuSn (278). One can safely assume strong covalent bonding within the hexagons that extend two-dimensionally in YbAuSn. The weaker interlayer gold−tin bonding interactions connecting the layers are quite longer (294 and 315 pm). The tin−tin interactions, however, are even shorter (298 pm) than those found in β-tin,[44] i.e., 4 × 302 pm and 2 × 318 pm in the form of a flattened tetrahedron with two additional tin atoms. The gold−gold contacts of 332 pm are in the range found for EuAuSn and CaAuSn, 335 and 326 pm, respectively, whereas they are shorter in EuAuGe (316 pm). In the latter compounds one surely has to consider the large relativistic contraction of the gold 6s orbitals[18] leading to gold−gold interactions.

Depending on the elemental combinations of the equiatomic AAuX compounds, *A* = electropositive element and X = main group element, one encounters different electronic situations paired with space requirements. The nature of the A and X elements influences the s electron density at the gold atoms and triggers consequently the various superstructures. The global minimum on the energy hypersurface is determined by an arrangement given by the KHg_2 type. Introducing secondary gold−gold and in the case of YbAuSn tin−tin bonding fine-tunes the structure. The latter can be held responsible for the formation of the superstructure of YbAuSn. The reason for the formation of the other KHg_2 type superstructures such as CaCuGe,[16] YPdSi,[45] and UPtGe[46] may be ascribed to similar secondary bonding interactions.

Acknowledgment. We are indebted to Prof. Dr. H. Eckert for his interest and steady support of this work. We also thank K. Wagner for the EDX analyses, Dipl.-Ing. U. Ch. Rodewald for some of the data collections, Dr. B. Künnen for the resistivity measurement, Dr. G. Kotzyba for the susceptibility measurement, and the Degussa-Hüls AG for a generous gift of gold wire. Financial support by the Deutsche Forschungsgemeinschaft and by the Fonds der Chemischen Industrie is gratefully acknowledged.

CM011089Q

(43) Nuspl, G., Polborn, K., Evers, J., Landrum, G. A., Hoffmann, R. *Inorg. Chem.* **1996**, *35*, 6922.

(44) Donohue, J. *The Structures of the Elements*; Wiley: New York, 1974.

(45) Prots', Yu. M., Pöttgen, R., Jeitschko, W. *Z. Anorg. Allg. Chem.* **1998**, *624*, 425.

(46) Hoffmann, R.-D., Pöttgen, R., Lander, G. H., Rebizant, J. *Solid State Sci.* **2001**, *3*, 697.

(47) Hoffmann, R.-D. *RWERT, Programe for the Calculation of Separate Residuals for Superstructure Reflections*; University of Münster, 1996.